



www.sciencemag.org/cgi/content/full/1131163/DC1

Supporting Online Material for
**Rapid Chemically Induced Changes of PtdIns(4,5)P₂ Gate
KCNQ Ion Channels**

Byung-Chang Suh, Takanari Inoue, Tobias Meyer, Bertil Hille*

*To whom correspondence should be addressed. E-mail: hille@u.washington.edu

Published 21 September 2006 on *Science Express*
DOI: 10.1126/science.1131163

This PDF file includes:

Materials and Methods
Figs. S1 to S6
References

Supporting Online Material

Materials and Methods

Cell culture, transfection and live-cell confocal imaging. Culture, transfection and imaging of NIH3T3 cells were performed as described (7). Briefly, cells were transfected with a solution containing DNA plasmids and Lipofectamine. Live-cell dual-color measurements were performed on a spinning-disc confocal microscope. Excitation lasers were processed with appropriate filter sets for CFP and YFP to capture cellular fluorescence images with a CCD camera, driven by Metamorph 4.6 imaging software (Universal Imaging). Fluorescence images of cells were taken every 10 s or 30 s at room temperature, depending on the experimental conditions. Human embryonic kidney tsA-201 (tsA) cells were cultured and transiently transfected using Lipofectamine 2000 with various cDNAs: M₁-muscarinic receptor (from Neil Nathanson, University of Washington, Seattle, WA), mRFP-PH(PLC δ) (RFP-PH(PLC δ), from C. Kearns, University of Washington, using mRFP from Roger Tsien, University of California, San Diego, CA), inositol 1,4,5-trisphosphate-5-phosphatase (InsP₃ 5-P, from M. Iino, University of Tokyo, Japan), CFP-FKBP (CF), CFP-FKBP-Inp54p (CF-Inp), Lyn₁₁-FRB (LDR), the channel subunits KCNQ2 and KCNQ3 (Kv7.2 and Kv7.3, from David McKinnon, State University of New York, Stony Brook, NY). TsA cells were maintained in DMEM supplemented with 10% FBS and 0.2% penicillin/ streptomycin and imaged 24–48 h after transfection on poly-L-lysine-coated coverslips. Images were taken every 5 s or 6.5 s on a Leica TCS/MP confocal microscope at room temperature and processed with Metamorph and Igor Pro 4.0. To obtain the time courses, the mean fluorescence intensity F over a given region of the cytosol or nucleus was measured.

Design of CFP-FKBP-enzyme constructs. Inp54p (a kind gift from Dr John York at Duke University, PubMed accession number; Z74807) (8) was subcloned into a previously developed CFP-FKBP plasmid (7). Specifically, Inp54p was subjected to PCR to provide EcoRI and BamHI cleavage sites at its 5' and 3' ends, respectively, and the PCR product was inserted into CFP-FKBP plasmid using EcoRI and BamHI restriction enzymes. Since the C-terminus of Inp54p serves as an ER targeting motif and truncation of this region leads to a cytosolic distribution of the protein, we removed it from Inp54p by placing a stop codon at position 331. The N-terminal 331 amino acids of Inp54p contain its catalytic domain and retain full phosphatase activity (S1). A phosphatase-dead version was made with a D281A mutation (13). For the construction of CFP-FKBP-PIPK (CF-PIPK), three types of modification were made in PtdIns(4)P-5-kinase type I γ (NM008844) (16). The C-terminus (636-661) was truncated to prevent localization to focal adhesions (18), R445E and K446E mutations were introduced to favor distribution to cytosol instead of plasma membrane (S2), and a S264A mutation was introduced to prevent phosphorylation, a known inactivating mechanism for this enzyme (S3). The resulting kinase was then subcloned into the CFP-FKBP plasmid using EcoRI and BamHI. The kinase-dead mutant (CF-PIPKi) had an additional D253A mutation (18) introduced using Stratagene QuickChange Site-Directed Mutagenesis. To construct CFP-FKBP-p85 (CF-iSH), the inter Src homology region 2 (iSH2, 420-615 aa) from p85 (a kind gift from Alliance for Cellular Signaling, BC006796) was subcloned into CFP-FKBP plasmid using XhoI and EcoRI after performing PCR reaction for iSH2 domain to have these restriction enzyme sites. In some experiments concerning PtdIns(3,4,5)P₃ tsA cells were first incubated for 15-20 hours in serum-free conditions as noted.

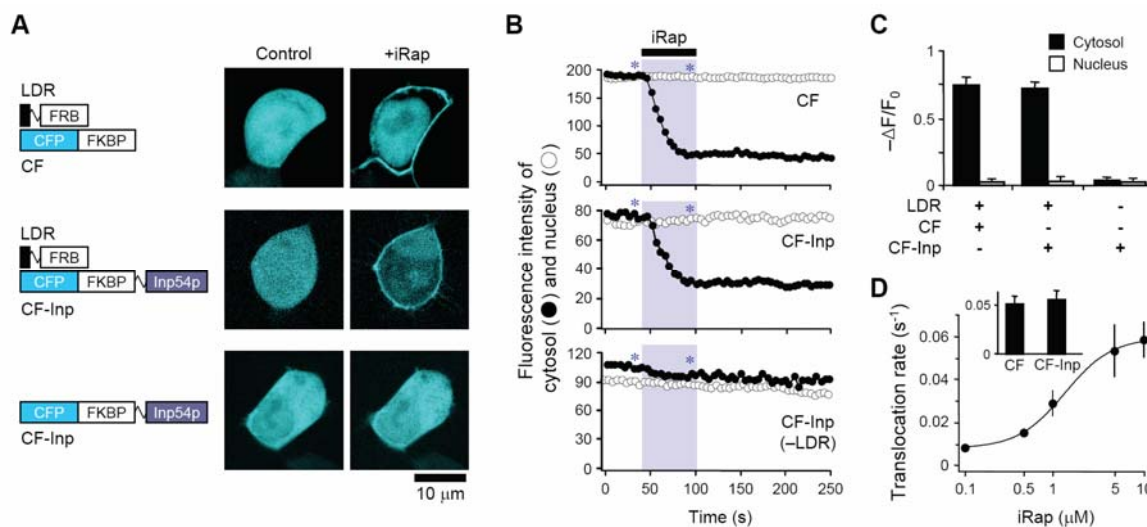


Fig. S1. Translocation of CFP-tagged FKBP to membrane-targeted FRB in tsA cells. **(A)** Confocal images of tsA cells expressing membrane localized Lyn₁₁-FRB (LDR) and cytosolic localized CFP-FKBP (CF) or CFP-FKBP-Inp54p (CF-Inp) before and after addition of iRap. Cells transfected either with LDR plus CF (top) or CF-Inp (middle), or with CF-Inp alone (bottom) were treated with iRap (5 μ M) for 1 min. **(B)** Fluorescence intensity of CF construct in cytosol (filled circles) and nucleus (open circles) during the addition of iRap. Time points indicated by asterisks correspond to the confocal images shown in **A**. Initially the

(C) Decrease of fluorescence intensity ($-\Delta F/F_0$) in cytosol and nucleus by iRap addition. Translocation of CF required the membrane anchor LDR but not the Inp54p enzyme. It is irreversible. **(D)** Rate constants of probe translocation to the plasma membrane with various iRap concentrations. Inset shows the rate constants (s^{-1}) of probe translocation in CF- and CF-Inp-expressing cells with 5 μ M iRap ($n = 3-8$). At high iRap concentration (5-10 μ M) the translocation rate constant was equivalent to a 14-s $t_{1/2}$. Mean and s.e.m.

nuclear and cytosolic CF concentrations are the same, and unlike EGFP-PH(PLC δ) and EGFP-PH(PLC δ) probes, the CF probes do not leave the nucleus within minutes after their cytosolic concentration falls (compare Ref. 13).

Electrophysiology. TsA cells were whole-cell clamped at room temperature 24–48 h after transfection (3). When measuring the rates of induction and recovery from muscarinic inhibition of the current, we applied test and control solutions rapidly to the 100 μ l chamber (flow rate of 1.5 ml min⁻¹) in the vicinity of the recorded cell. Cells were held at a holding potential of -20 mV, and 500-ms test pulses to -60 mV were given every 4 s. Reported values (I_{-20} mV) are mean outward current taken at -20 mV just before each step to -60 mV. Recordings started ~5 min after breakthrough. Voltage dependence of activation was measured from the relative amplitudes of tail currents at -70 mV following depolarizing test pulses to various test potentials.

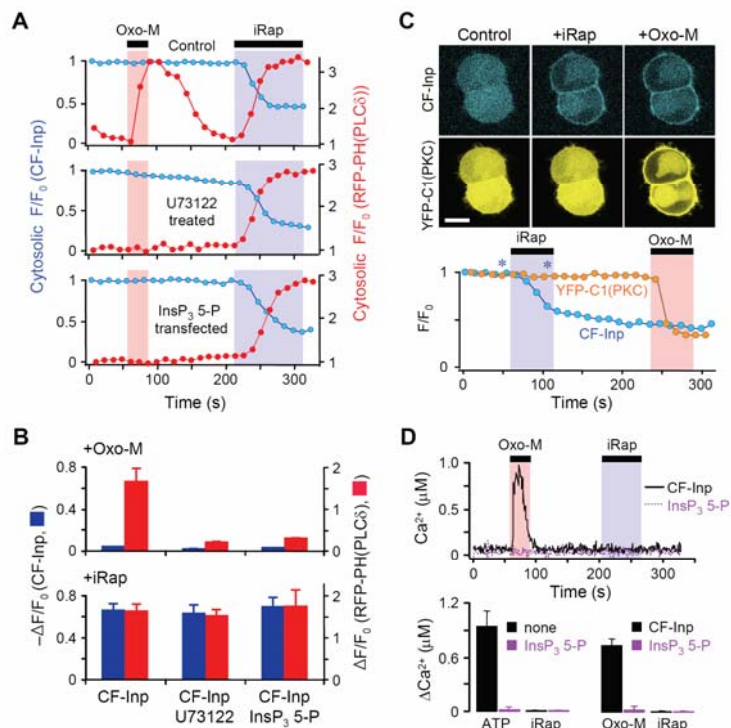


Fig. S2. Inositol polyphosphate 5-phosphatase (Inp54p) translocation and intracellular signals in tsA cells. **(A)** Translocation of CFP-tagged CF-Inp (blue) and the RFP-tagged PH domain of PLC δ 1 (RFP-PH(PLC δ)) (red) upon addition of Oxo-M (10 μ M) or iRap (5 μ M). The measurements are from two-wavelength confocal images of tsA cells also transfected with M₁R (top) and treated with the PLC inhibitor U73122 (3 μ M) (middle) or co-expressing InsP₃ 5-phosphatase (InsP₃ 5-P) (bottom). Interestingly, these results show that the YFP-PH(PLC δ) probe responds well to large changes of PtdIns(4,5)P₂ when InsP₃ is not changing from its resting value. **(B)** Changes of fluorescence intensity (F/F_0) of CF-Inp (blue) and RFP-PH(PLC δ) (red) in the cytosol upon addition of Oxo-M or iRap ($n = 3-5$). Mean and s.e.m. **(C)** Dual confocal images of CF-Inp and YFP-tagged C1 domain of protein kinase C γ 1 (YFP-C1(PKC)) before and after addition of iRap and Oxo-M (upper panels). Scale bar, 10 μ m. Time course of fluorescence intensity (F/F_0) of CFP and YFP in cytosol during addition of iRap and Oxo-M (bottom panel). Asterisks indicate time points corresponding to the confocal images shown in upper panels. **(D)** No effect of iRap on intracellular Ca^{2+} levels. Upper panel, typical Ca^{2+} traces (fura-2) in cells transfected with CF-Inp (solid line) or CF-Inp plus InsP₃ 5-P (dotted line). Bottom panel, summary of intracellular Ca^{2+} changes by ATP (100 μ M) (acting on endogenous purinergic receptors), Oxo-M (10 μ M), or iRap (5 μ M) in the tsA cells with or without expressed CF-Inp and with or without InsP₃ 5-P ($n = 6$). Mean and s.e.m.

Statistics. Where relevant, histograms and data are given as mean \pm s.e.m.

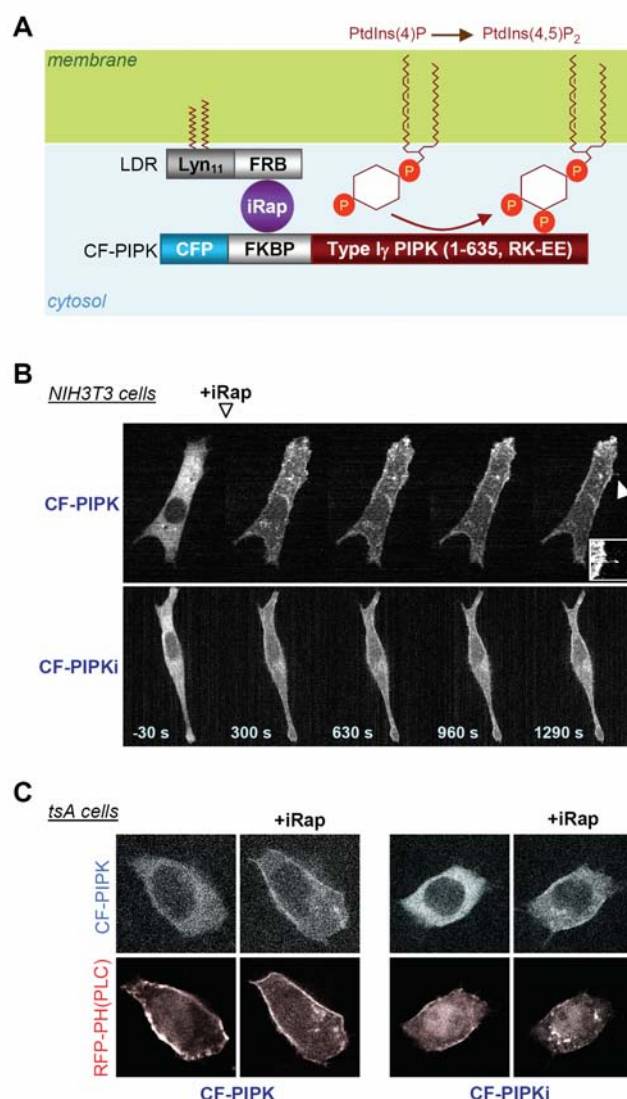


Fig. S3. Translocation of PtdIns(4)P-5-kinase type I γ (PIPKI γ) in NIH3T3 and tsA cells. **(A)** Schematic of translocatable PIPKI γ system dimerized by iRap. Membrane recruitment of CF-PIPK by iRap induces specific phosphorylation at the 5-position of PtdIns(4)P to make PtdIns(4,5)P₂. **(B)** Time-series confocal fluorescent images (CFP wavelength) taken at 5-min intervals of NIH3T3 cells expressing Lyn₁₁-FRB (LDR) plus CF-PIPK (1-635, RK-EE) or kinase dead mutant CF-PIPKi (1-635, RK-EE, D253A). iRap was added between the first and second images. Arrow indicates a protrusion frequently formed after translocation of active CF-PIPK but not CFPIPKi (Inset: Enlargement of protrusion). **(C)** Confocal CFP and RFP images before and after 1 min addition of iRap (5 μ M) to tsA cells expressing LDR, RFP-PH(PLC δ), and either CF-PIPK or CF-PIPKi. iRap induced rapid translocation of CFP constructs to the membrane but had little effect on the distribution of RFP-PH(PLC δ), which was already reporting a high resting concentration of PtdIns(4,5)P₂ at the plasma membrane.

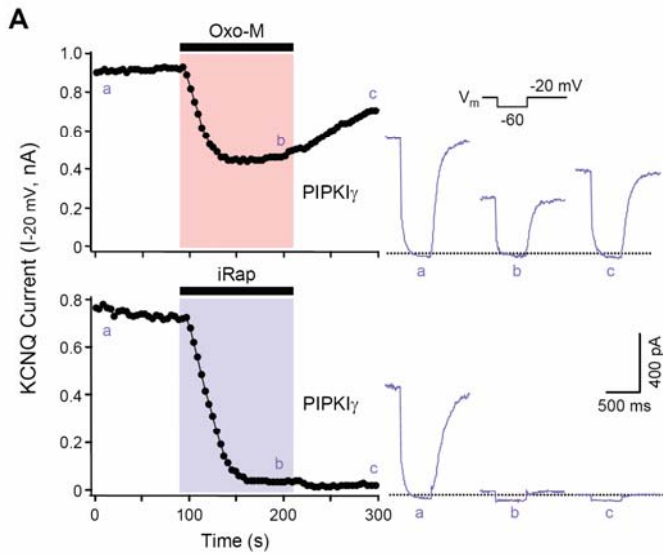


Fig. S4. Expression of wild-type PtdIns(4)P-5-kinase type I γ (PIPKI γ) slows and reduces modulation of KCNQ current by iRap and Oxo-M. **(A)** Effect of Oxo-M (upper panels) or iRap (bottom panels) on KCNQ2/KCNQ3 channel activity in tsA cells expressing full-length wild-type PIPKI γ and the LDR/CF-1np-translocation system. Insets show current waveforms at times before and after application of iRap and Oxo-M. Dotted line is the zero-current level. **(B)** Summary of the current-inhibition time constants and % inhibition by iRap and Oxo-M ($n = 5$). Mean and s.e.m.

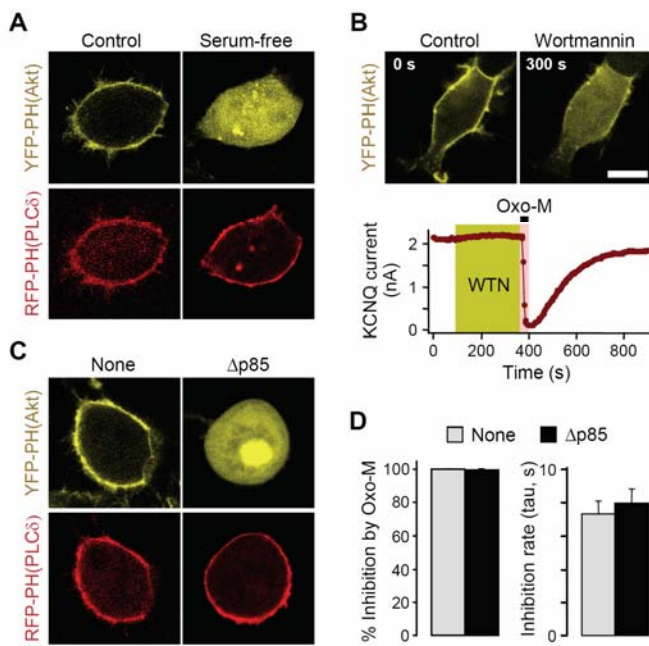


Fig. S5. Plasma membrane PtdIns(3,4,5)P $_3$ does not affect KCNQ current in tsA cells. **(A)** Dual confocal images of the indicator probes, YFP-tagged PH(Akt) (YFP-PH(Akt)) and RFP-tagged PH domain of PLC δ 1 (RFP-PH(PLC δ)), show that normally cultured tsA cells have PtdIns(3,4,5)P $_3$ and PtdIns(4,5)P $_2$ in the plasma membrane. Culturing in serum-free medium for 15-20 hr translocates YFP-PH(Akt) but not RFP-PH(PLC δ) to the cytosol, indicating loss of PtdIns(3,4,5)P $_3$ and little change of PtdIns(4,5)P $_2$ level in the plasma membrane. **(B)** The PtdIns-3-kinase inhibitor wortmannin (300 nM) translocates YFP-PH(Akt) to the cytosol, showing that PtdIns-3-kinase is active in normally cultured tsA cells. Scale bar, 10 μ m. Bottom panel, 5-min addition of wortmannin (500 nM) changes neither the amplitude of KCNQ current nor the Oxo-M-induced modulation. **(C)** Overexpressing the dominant negative PtdIns-3-kinase mutant ($\Delta p85$) induces translocation of YFP-PH(Akt) to the cytosol without any significant effect on the RFP-PH(PLC δ). **(D)** Percent inhibition of KCNQ current by Oxo-M and the time constant of inhibition.

Expression of $\Delta p85$ does not change modulation of KCNQ channels by Oxo-M ($n = 5$). Mean and s.e.m.

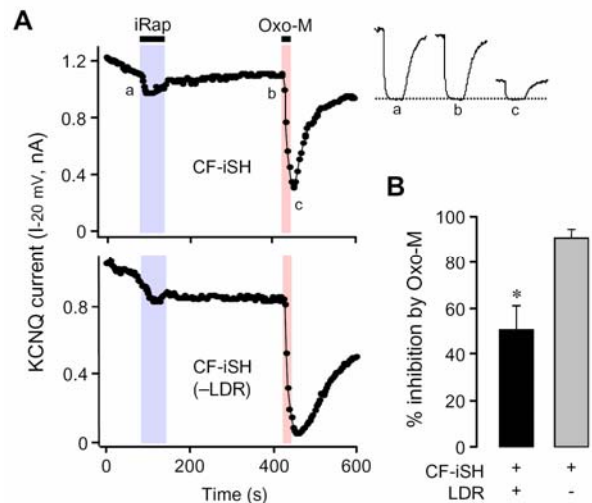


Fig. S6. iRap-induced translocation of PtdIns-3-kinase diminishes the subsequent suppression by Oxo-M. **(A)** Modulation after iRap application of KCNQ2/KCNQ3 current by Oxo-M (10 μ M) in single tsA cells expressing CF-iSH with (left) or without (right) LDR constructs. These cells were cultured overnight in serum-free conditions. **(B)** Summary of muscarinic modulation of KCNQ current. Maximum percent inhibition after application of Oxo-M for 20 s. * Significant difference at 1% level ($P = 0.0074$; $n = 4$). Mean and s.e.m.

References for Supporting Material

S1. F. Wiradjaja et al., *J. Biol. Chem.* **276**, 7643 (2001).
 S2. M. Arioka, S. Nakashima, Y. Shibasaki, K. Kitamoto, *Biochem. Biophys. Res. Comm.* **319**, 456 (2004).
 S3. Y. Aikawa, T. F. Martin, *J. Cell Biol.* **162**, 647 (2003).